



Article

Evaluating the Ability of FARSITE to Simulate Wildfires Influenced by Extreme, Downslope Winds in Santa Barbara, California

Katelyn Zigner ^{1,*}, Leila M. V. Carvalho ^{1,2}, Seth Peterson ¹, Francis Fujioka ³, Gert-Jan Duine ², Charles Jones ^{1,2}, Dar Roberts ^{1,2} and Max Moritz ^{1,2,4}

¹ Department of Geography, University of California, Santa Barbara, Santa Barbara, CA 93106, USA; leila@eri.ucsb.edu (L.M.V.C.); seth@geog.ucsb.edu (S.P.); cjones@ucsb.edu (C.J.); dar@geog.ucsb.edu (D.R.); mmoritz@ucsb.edu (M.M.)

² Earth Research Institute, University of California, Santa Barbara, CA 93106, USA; duine@eri.ucsb.edu

³ CEESMO, Chapman University, Orange, CA 92866, USA; fujitoo2@yahoo.com

⁴ University of California Cooperative Extension, Agriculture and Natural Resources Division, Oakland, CA 94607, USA

* Correspondence: kzigner@ucsb.edu

Received: 12 June 2020; Accepted: 7 July 2020; Published: 10 July 2020



Abstract: Extreme, downslope mountain winds often generate dangerous wildfire conditions. We used the wildfire spread model Fire Area Simulator (FARSITE) to simulate two wildfires influenced by strong wind events in Santa Barbara, CA. High spatial-resolution imagery for fuel maps and hourly wind downscaled to 100 m were used as model inputs, and sensitivity tests were performed to evaluate the effects of ignition timing and location on fire spread. Additionally, burn area rasters from FARSITE simulations were compared to minimum travel time rasters from FlamMap simulations, a wildfire model similar to FARSITE that holds environmental variables constant. Utilization of two case studies during strong winds revealed that FARSITE was able to successfully reconstruct the spread rate and size of wildfires when spotting was minimal. However, in situations when spotting was an important factor in rapid downslope wildfire spread, both FARSITE and FlamMap were unable to simulate realistic fire perimeters. We show that this is due to inherent limitations in the models themselves, related to the slope-orientation relative to the simulated fire spread, and the dependence of ember launch and land locations. This finding has widespread implications, given the role of spotting in fire progression during extreme wind events.

Keywords: wildfire modeling; FARSITE; spotting; fire weather; Sundowner winds

1. Introduction

Around the world, destructive wildfires significantly disrupt lives through personal and economic losses, degraded air quality [1], and an enhanced risk of landslides and debris flows [2]. Understanding future climatic and anthropogenic changes that will alter wildfire season and intensity is crucial for highly-populated and at-risk locations such as southern California communities. Wet winters and dry summers in this climate lead to a wildfire season generally between May and October, although rising temperatures associated with climate change will advance fuel drying and extend the length of the fire season [3–5]. Furthermore, projected increases of extreme meteorological events such as heat waves [6] will affect the frequency, severity, and spatial distribution of wildfires. Combined with the expected changes in the regional climate, the probability of impactful wildfires may increase in the future in coastal Santa Barbara due to an increasing number of ignitions from expansion of the wildland-urban interface [7–10].

Wildfire behavior is determined by fuels, topography, and weather [11], commonly called the “fire behavior triangle” or the “fire environment triangle”. In the case of extreme wind events, meteorological conditions are the leading factor that determines wildfire spread and intensity [12–18]. Extreme, downslope wind events in coastal Santa Barbara County are called “Sundowner winds” (or “Sundowners”) due to the onset of gusty winds around sunset [19,20]. Sundowners are most frequent in spring [21,22] when fire danger is relatively low, but they can occur year-round. These events may produce critical fire weather conditions throughout the evening, including gale-force winds and relative humidity below 15% [23,24]. Some of these events have been associated with abnormally high temperatures in the evening occasionally exceeding 30 °C after sunset during summer [19,20].

While strong wind events may create extreme fire weather conditions and cause rapid wildfire spread, no previous studies have placed emphasis on examining the sensitivity of operationally-used wildfire models to simulate wildfires significantly influenced by downslope wind events. This is important because Sundowners have rapidly spread all major wildfires on the south side of the Santa Ynez Mountains (SYM) toward a coastal community of ~150,000 inhabitants [25] (Figure 1). All abbreviations used in this paper are listed in Table A1, and statistics for all major wildfires are shown in Table 1. Among those remarkable wildfires was the Painted Cave fire (June 1990), which quickly spread through dense, flammable vegetation driven by strong (~26 m/s) winds [19,24]. Between 2016 and 2019, Sundowners rapidly spread three major wildfires in coastal Santa Barbara County: the Sherpa (June 2016), Thomas (December 2017), and Cave (December 2019) fires. Northwesterly winds around 18 m/s rapidly spread the Sherpa Fire down the sparsely inhabited western slopes of the SYM. Driven by Sundowner winds, the Thomas Fire spread into the SYM and claimed the title of the largest southern California wildfire to date. Although wildfires have undeniably affected the inhabitants and ecosystem in this region, only one study so far [26] has attempted to reconstruct wildfires in coastal Santa Barbara County using wildfire models.

Wildland fire models such as the Fire Area Simulator (FARSITE) [27] and FlamMap [28,29] are used operationally to simulate prescribed burns in the national parks in the United States [30–32], and examine model sensitivity to fuel models and fuel moisture [33,34]. Additionally, these models provide decision support regarding appropriate responses on wildfire incidents [35], and FARSITE is typically selected to answer questions regarding fire size, location, and timing [29,35]. FARSITE and FlamMap are two-dimensional semi-empirical wildfire models that describe how surface wind flow spreads fire at fire line and geographical scales. These are uncoupled wildfire models because they do not consider interactions between the fire and the atmosphere, i.e. the feedback that occurs between the fire and local wind flow. The simplicity in the treatment of fuels, topography, and weather as independent variables is a limitation of uncoupled wildfire models, since these factors can greatly impact observed fire behavior [36]. In contrast, atmospheric models, such as the Weather Research and Forecasting model (WRF) [37] may be combined with fire-spread models (e.g. WRF-Fire [36] and WRF-SFIRE [38]) to describe this coupling at fire scales (i.e. tens of meters). Although highly sophisticated, these coupled models are computationally expensive and rarely used operationally [27,39]. Our choice to use uncoupled wildfire models is justified by the simplicity and quick simulation run time, which would be beneficial in an operational setting. The rapid simulation time is especially critical for fires in the Wildland-Urban Interface (WUI) for wildfire management and evacuation planning purposes. More information on the use, advantages, and disadvantages of FARSITE and FlamMap can be found in [32].

The ability of uncoupled fire spread models, such as FARSITE and FlamMap, to simulate downslope wildfire spread driven by extreme, downslope winds in the Santa Barbara area has not yet been assessed. Moreover, evacuation planning can become critical during wind-driven wildfires in Santa Barbara; thus, advancing research on wildfire spread and risk with operational models is essential. The overarching goal of this research is to examine the skill of FARSITE in simulating downslope fire spread under extreme conditions by focusing on two of the most rapidly spreading wildfires that have affected the southern slopes of the SYM during Sundowners. Additionally, burn

area rasters from simulations in FARSITE are further compared with the minimum travel time rasters from FlamMap simulations. The successful simulation of wildfire case studies using uncoupled fire spread models such as FARSITE with focus on spatiotemporal wind variability may allow for the creation of burn probability maps for fire risk assessment during Sundowners. This research may contribute to enhanced wildfire resource allocation and preparedness during extreme fire weather conditions. This study is organized as follows. Data sets, material, and methods are discussed in Section 2. Results and conclusions are presented in Section 3. Final conclusions are summarized in Section 4. A list of acronyms and the other figures are included in the Appendix A.

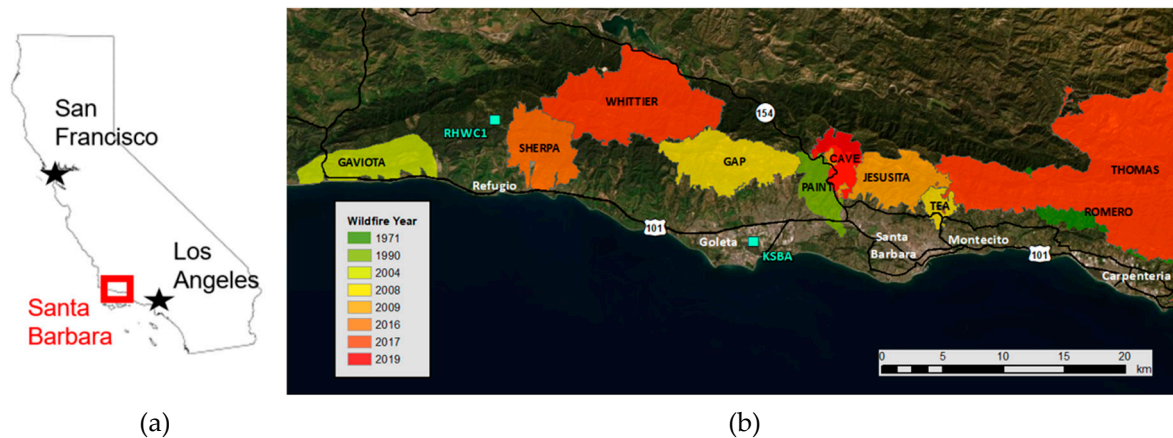


Figure 1. Region of interest (red rectangle; **a**) and perimeters of past wildfires in coastal Santa Barbara County between 1970 and 2019 (**b**), colored by the year of occurrence. The “PAINT” Fire is the Painted Cave Fire examined in this study. The thick, black lines indicate major roads and freeways (Highway 101 and Highway 154), and the two blue squares indicate weather stations used in this analysis.

Table 1. Information on past wildfires in coastal Santa Barbara County. It should be noted that the Thomas Fire ignited to the east of Santa Barbara in Ventura County and spread west in the first two weeks after ignition. The numbers in the table are from official reports that incorporate areas in coastal Santa Barbara. Additionally, the structural impacts, injuries, and deaths associated with the Montecito debris flow caused by the Thomas Fire were not included.

| Fire | Date | Acres Burned | Structural Impacts | Injuries and Deaths |
|--------------|---------------|--------------|--------------------|---------------------|
| Painted Cave | June 1990 | 2000 ha | 427 destroyed | 1 death |
| Tea | November 2008 | 785 ha | 210 destroyed | - |
| Jesusita | May 2009 | 3500 ha | 80 destroyed | - |
| Sherpa | June 2016 | 3200 ha | 1 destroyed | 1 injury |
| Thomas | December 2017 | 110,000 ha | 1000 destroyed | 2 deaths |
| Cave | November 2019 | 1265 ha | - | - |

2. Materials and Methods

2.1. Case Studies

Two wildfires rapidly spread by Sundowner winds were selected to test the ability of FARSITE to reconstruct fires perimeters during extreme fire weather conditions. The first case study, the Sherpa Fire, was selected because of the availability of a high-resolution fuel map from remotely sensed data taken approximately two years before the fire, and multiple fire perimeters obtained in the hours after ignition, allowing for numerous comparisons of observed and simulated fire perimeters. The fire ignited at 1515 Pacific Daylight Time (PDT) on 15th June 2016 in the slopes of western SYM along the Gaviota Coast in Santa Barbara County from embers blown off a burning log. Sundowner winds on the first night of the fire rapidly spread the fire southward down canyons. Winds were strong at the nearby Refugio station (RHWC1; see Figure 1 for location), ranging 16–18 m/s on the evening of the fire.

North-northwesterly winds recorded at a station downhill (south) were less than 10 m/s, illustrating the limited spatial extent of the Sundowner event [22]. At the time of ignition, RHCW1 reported a temperature of 19 °C and relative humidity of 38% with no temperature ramps or sudden drops in moisture evident in the following hours. Strong, northerly winds and gusts reaching 23 m/s continued throughout the night and rapidly spread this fire south, resulting in evacuations and the closure of Highway 101 (Figure 1).

The second case study was chosen because of exceptionally fast fire spread from Sundowner winds and the significant influence on populated areas. The arson-caused Painted Cave Fire ignited on June 27th, 1990 at 1800 PDT off Highway 154, close to the SYM ridgeline (Figure 1). In addition to an extended three-to-four-year drought, temperatures exceeding 38 °C and relative humidity values below 20% in the three-day heat wave preceding the fire left the dense chaparral dry and very flammable [19]. Extreme winds and gusts launched burning branches and flaming embers ahead of the fire front and spread the fire downhill toward urban Santa Barbara, travelling 3 km in the first 20 min and 6 km to Highway 101 in 1 h [19,40]. Additionally, backfiring operations spread the fire eastward across Highway 154, and an upslope (southerly) wind shift spread the fire northwest of the ignition point on the second day.

2.2. Wildland Fire Models

Wildfires were simulated using the vector-based, deterministic fire model FARSITE v4 built within FlamMap6. FARSITE uses Huygen's principle of wave propagation and the Rothermel fire spread equations [12] to simulate fire spread creating a series of ellipses at multiple vertices on the fire front [27,41]. Surface and crown fires are separated and use the Rothermel [12] and Van Wagner [42] models, respectively. FARSITE uses Albini's equations [43] for spotting from torching vegetation and calculates the maximum distance an ember can travel using wind speed, topography, and ember size, shape, and density [27]. Additionally, wind speed is considered only horizontally, and is assumed to increase logarithmically with height above the 6.1 m (20 ft) input winds [27]. Required inputs include elevation, slope, aspect, fuel model, canopy cover, crown base height, and crown bulk density, and meteorological data, including temperature, relative humidity, horizontal wind speed and direction, and precipitation.

FlamMap is another operationally-used, uncoupled wildfire model that shares many similarities with FARSITE, including the same input data (e.g. fuel map, crown base and stand height, bulk crown density, elevation, aspect, slope, temperature, humidity, wind speed and direction, precipitation). The main difference between FARSITE and FlamMap is the absence of time-varying winds and fuel moisture conditions in FlamMap. The Minimum Travel Time (MTT) model calculates fire behavior at every grid cell and independent of one another, providing great use for comparisons of landscape treatment processes [32]. More information on the differences between FARSITE and FlamMap can be found in [44].

2.3. Fuel and Topography Data

Vegetation in southern California is primarily comprised of evergreen sclerophyllous shrubs, such as chamise and Ceanothus, as well as drought deciduous coastal sage scrub [45,46]. Both are well adapted to the long, dry summers and are highly flammable [15,47,48]. In our study, canonical discriminant analysis and linear discriminant analysis were applied to an 18 m Airborne Visible/Infrared Imaging Spectrometer (AVIRIS) image from 2014 for the Sherpa Fire [49], and 12 m from 2004 AVIRIS image for the Painted Cave Fire [50]. The 15-year gap between the Painted Cave fire and the 2004 imagery for the Painted Cave fire is likely enough time for the recovering vegetation to mimic the conditions at the time of the fire [51]. The classified images were cross-walked into fuel models from Anderson's original 13 fire behavior fuel models [41], Scott and Burgan's fuel models [52], and Weise and Regelbrugge's chaparral models [53]. Fuel model specifications are shown in Table 2 and Figure 2a,c. These materials are available upon request to the corresponding author.

Table 2. Fuel model information.

| Vegetation Name | Fuel Model Number | Fuel Model Source | Fuel Model Name | Fuel Model Code |
|--------------------|-------------------|-----------------------|-----------------------------------|-----------------|
| Short Grass | 1 | Anderson | - | - |
| Chamise | 15 | Weise and Regelbrugge | - | - |
| Ceanothus | 16 | Weise and Regelbrugge | - | - |
| Coastal Sage Scrub | 18 | Weise and Regelbrugge | - | - |
| Suburban/WUI | 23 | Scott and Burgan | Moderate Load Conifer Litter | TL3 |
| Shrubs | 145 | Scott and Burgan | High Load, Dry Climate Shrub | SH5 |
| Dense Shrubs | 147 | Scott and Burgan | Very High Load, Dry Climate Shrub | SH7 |
| Trees/Riparian | 162 | Scott and Burgan | Timber-Understory | TU2 |

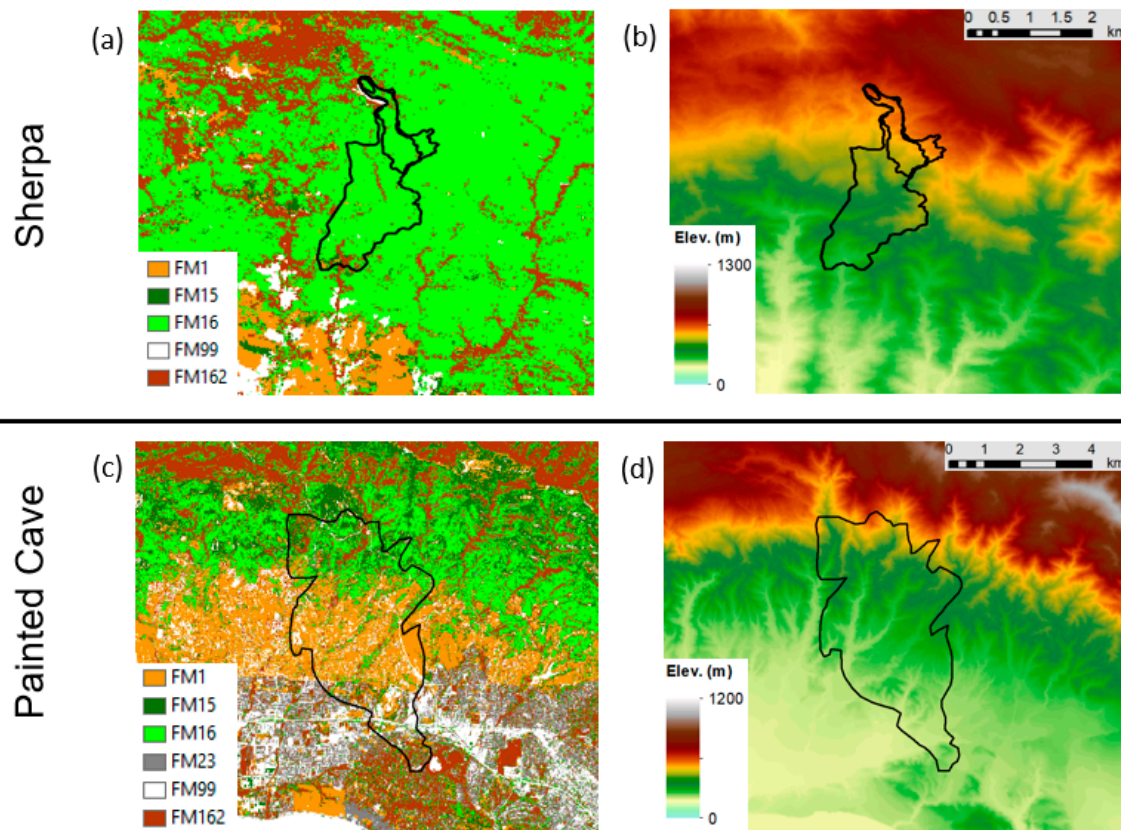


Figure 2. Fuel maps (a,c) and elevation (b,d) rasters for the Sherpa (a,b) and Painted Cave (c,d) fires. The black polygons are the fire perimeters at 1600, 1800, and 1900 PDT for the Sherpa Fire, and the final perimeter for the Painted Cave Fire. Fuel type numbers and names are indicated in Table 2.

Minor modifications in burnable and unburnable classifications were applied to the fuel maps for both case studies; the area south of the Sherpa Fire ignition is a campsite (Rancho La Scherpa) with a combination of sparse and irrigated vegetation. Hence, this region was classified as unburnable. The Painted Cave Fire spread southward into suburban and urban Santa Barbara, which were originally classified as unburnable, limiting the potential extent of the simulated fire spread. A dense timber-litter fuel model was chosen for suburban areas to imitate these regions with intermingled vegetation and buildings. Areas consisting of primarily concrete roads and stucco structures considered ‘urban’ remained classified as unburnable.

Elevation data at 30 m spatial resolution acquired from the Shuttle Radar Topography Mission [54] was used for the FARSITE elevation, slope, and aspect rasters for each case study (Figure 2b,d).

2.4. Weather Data

Given the narrow SYM (10 km) and limited availability of surface weather stations, atmospheric data were obtained with WRF simulations at 1 km grid spacing. For our case studies, hourly 1 km gridded 2 m temperature, 2 m relative humidity, and 10 m wind (east-west and north-south components) were created using the WRF with the configuration specified in [55].

Hourly temperature, relative humidity, and precipitation data from a selected point were input to FARSITE through a weather stream file [56] created using WRF data and applied over the entire domain. In coastal Santa Barbara County, there are significant gradients in weather conditions between the SYM slopes and areas near the coast [55,57]. Therefore, the location used for the weather stream file data must be representative of conditions close to the fire. For these two case studies, we created weather stream files using the WRF grid cell closest to the ignition sites.

Wildfire spread is exceedingly sensitive to local winds, especially extreme winds [12,14,57], and the utilization of gridded wind data in wildfire modeling has improved the agreement between simulated and observed perimeters [18,58,59]. Mass-conserving meteorological wind downscalers such as WindNinja [60,61] have been used to increase resolution of gridded winds and have produced more accurate fire perimeters in FARSITE and FlamMap in some case studies [28,34,62–64]. To capture the variability of winds over the complex terrain in coastal Santa Barbara County, the 1 km WRF wind output was downscaled to 100 m using WindNinja (henceforth “WN”). This software requires an elevation raster and single-point or gridded wind data, and outputs wind speed and direction in raster format. Figure 3 illustrates differences in winds as a consequence of different grid spacing at 1 km (WRF) compared to 100 m (WN) at the time of ignition for the Sherpa and Painted Cave fires. Smoothing effects as a consequence of the grid spacing at 1 km (WRF) and 100 m (WN) will influence simulated fire spread. It is also important to note the height differences between the 10 m agl WRF surface wind files and the 6.1 m agl WN surface wind files.

To determine potential errors associated with temperature, relative humidity, and wind speed, we compared station observations acquired from Mesowest [65] with the closest WRF and WN (for wind speed only) grid cell for each case study (Figure 4). We compared model output with RHWC1 during the Sherpa Fire because of its close proximity to the fire. The Santa Barbara airport station (henceforth KSBA; see Figure 1 for location) was the only weather station installed during the Painted Cave fire, and was thus used to validate meteorological variables. This station did not archive data in the early morning hours, resulting in breaks in station data (Black lines in Figure 4d–f). RHWC1 is a Remote Automatic Weather Station (RAWS) owned by the U.S. Forest Service, whereas KSBA is an Automated Surface Observing System owned by the National Weather Service. It's important to note that RHWC1 records all wind measurements at 6.1 m agl and non-wind measurements (e.g. temperature, relative humidity) at 2 m agl. KSBA measures wind at 10 m agl and measures non-wind variables at 2 m agl. WRF surface files were bilinearly interpolated to 2 m for temperature and relative humidity, and 10 m agl for wind, whereas WN produces wind rasters at 6.1 m agl.

Although there was generally high agreement in wind speed between the WRF and WN grid cells (Figure 4), we observe biases in temperature and relative humidity between WRF and stations; RAWS are usually placed in locations that are normally exposed to high wind speeds, other near canyons and passes. These topographic features are mostly smoothed in 1 km grid simulations, largely explaining differences in wind speeds between model output and station observations. Biases between WRF and KSBA have been shown in previous studies [24,55,57] and are attributed to the station's proximity to the ocean, and the representation of the transition between the marine and coastal boundary layer in simulations. The choice of WRF parameterizations and implications for simulations are discussed in [55].

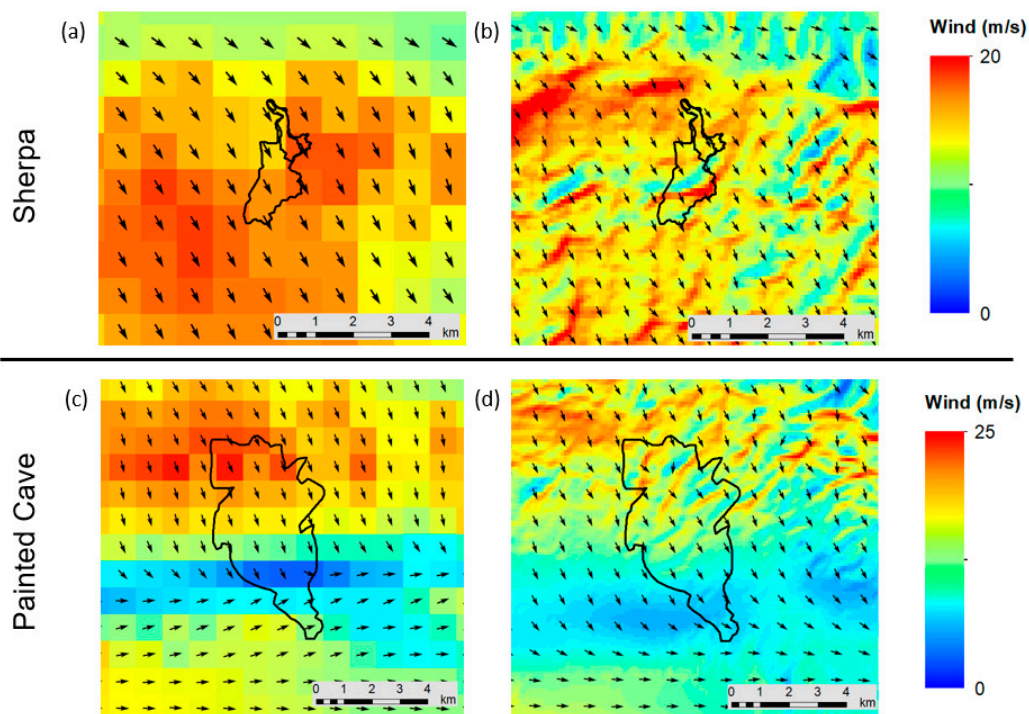


Figure 3. Examples of gridded wind data from WRF at 1 km resolution (a,c) and WN at 100 m resolution (b,d) at the time of ignition for the two wildfire case studies. It’s important to note that output is at 10 m (~30 ft) for the WRF surface winds and at 6.1 m (20 ft) for WN surface winds used in this analysis. The black polygons are the fire perimeters at 1600, 1800, and 1900 PDT for the Sherpa Fire, and the final perimeter for the Painted Cave Fire.

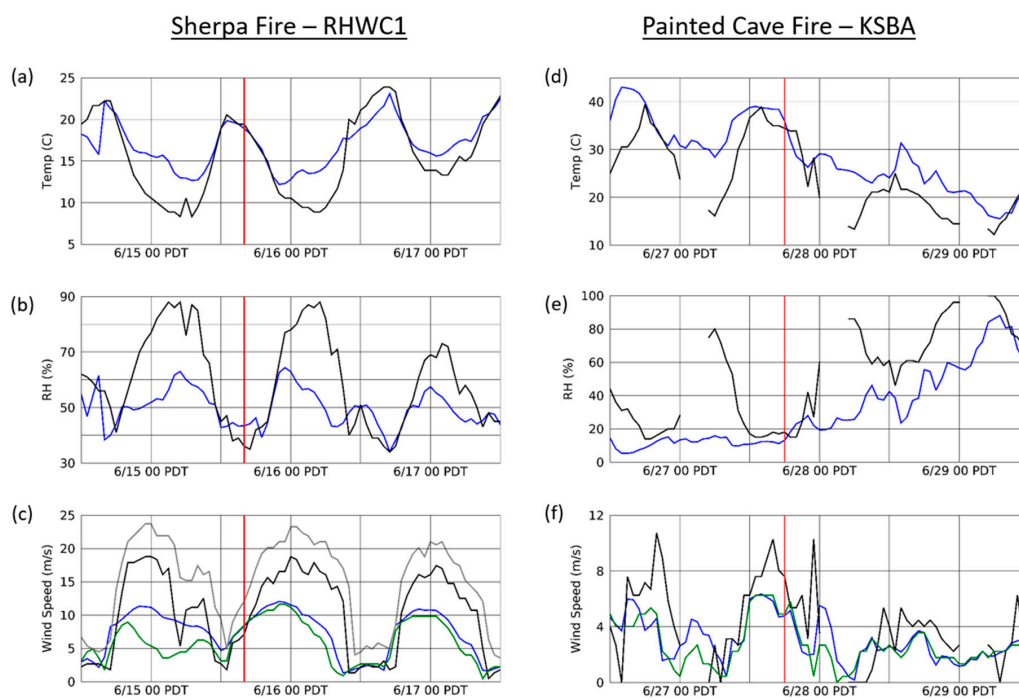


Figure 4. Observed (black) and simulated with WRF (blue) temperature (a,d), relative humidity (b,e), and wind (c,f) at the nearest weather stations for the Sherpa (RHWC1) and Painted Cave (KSBA) fires. WindNinja data was added for wind plots (green lines in (c,f)) and observed gust data was available at RHWC1 (grey line in (c)). The vertical red line indicates the time of ignition for each fire.

Interestingly, the simulated temperature and relative humidity values around the ignition times were fairly close to observations during both case studies (Figure 4a,b,d,e). WRF and WN underestimated wind speeds, and this difference was largest in the evening during the Sherpa Fire (Figure 4c) when the observed winds were ~5 m/s higher and observed wind gusts were more than 10 m/s higher than simulated winds. During the Painted Cave fire, simulated winds typically underestimated KSBA wind speeds by less than 2 m/s (Figure 4f). The underestimation of simulated winds at these grid cells may produce underestimations in simulated fire perimeters.

2.5. Gust Factor

Wind gusts play a crucial role in wildfire spread, intensity, and spotting [12,29,66], but are not simulated by WRF. As suggested in [67], gusts provide value for understanding extreme winds from an observational and wildfire-focused standpoint based on differing calculation methods. Wind speeds reported at RAWS such as RHC1 are the average of winds in the 10-min prior to every hour, whereas gusts are the maximum wind recorded in the previous hour. Previous studies [67–70] utilized station observations to create a wind gust approximation termed the ‘gust factor’. The gust factor (GF) is calculated by dividing the gust speed by the wind speed, and varies between stations due to sampling length and frequency, averaging interval, and instrument mounting height [70].

To mimic the effect of gusts on simulated wildfire spread, we applied a GF to WN rasters. We chose to apply a gust factor to the WN gridded wind files because WRF and WN underestimated winds in both case studies (Figure 4c,f). Underestimates of wind speed will result in underestimated fire spread. However, the spatiotemporal variability of wind gusts is difficult to simulate, and the application of a constant GF over the domains and at all times may lead to overestimated fire spread.

Wind gust data were not available during the Painted Cave Fire, but were available during the Sherpa Fire at RHC1 (Figure 4c). At the time of ignition for the Sherpa Fire, the GF was 1.71, although increased wind speeds and gusts later in the evening decreased the GF to 1.28 at 1800 PDT. The average GF between the time of ignition and the last observed perimeter of that first evening (1500 to 1900 PDT) was 1.38, demonstrating the variability of the GF through the use of different temporal subsets. While GFs have not been extensively analyzed in coastal Santa Barbara, studies on Santa Ana and Diablo winds calculated an average GF of 1.7 [67–69]. In this study, the Sherpa and Painted Cave fires were simulated multiple times using no gust factor, a 1.4 GF, and a 1.7 GF. We then compared the simulated and observed fire perimeters using these differing wind inputs.

2.6. Perimeter Data

Perimeter data for both fires are available from the Santa Barbara County Fire Department [71]. The Sherpa Fire has observed perimeters at 1600, 1700, 1800, and 1900 PDT. Only one, the final perimeter, is available for the Painted Cave Fire, although the southward fire spread rate and parts of the fire perimeter were estimated from recollections (see Case Studies Section).

Simulated and observed perimeters were quantitatively analyzed using the Sorensen metric (SM) [72,73], defined as:

$$SM = 2a / (2a + b + c)$$

where *a* is the area burned by both the observed and simulated fires, *b* is the area burned by only the observed fire, and *c* is the area burned by only the simulation. SM values closer to 0 indicate little agreement between observed and simulated perimeters, and values closer to 1 indicate high agreement. This metric has been used to compare wildfire perimeters in [31,74–76].

3. Results and Discussion

3.1. Sherpa Fire

Figure 5 shows observed and simulated perimeters for the Sherpa Fire, with simulations run applying no GF (henceforth 1.0 GF), a 1.4 GF, and a 1.7 GF. All FARSITE simulations used the vegetation

and spotting specifications in Table 3 and started at 1500 PDT. The area burned and SM values for the observed perimeters and all simulations are shown in Table 4. After one hour (at 1600 PDT), the 1.0 GF simulation had best agreement with observed perimeters in terms of fire shape and size, but greatly underestimated all other perimeters later in the evening (Figure 5a). At 1700 PDT, the 1.4 GF simulation underestimated the perimeter (Figure 5b) and the 1.7 GF simulation overestimated the perimeter (Figure 5c), notably resulting in equal SM values for different reasons. At 1800 PDT, the 1.4 GF simulation had the highest SM value (0.64; see Table 4) and highest agreement in burned area of all simulations at this time. While the 1.4 GF simulation had the highest SM value at 1900 PDT, all GF simulations underestimated the total amount of area burned (Table 4). The 1.7 GF simulation had the closest amount of burned area to that observed, underestimating by less than 10 ha. The higher SM value for the 1.4 GF simulation is explained by the reduction of area burned compared to the 1.7 GF simulation.

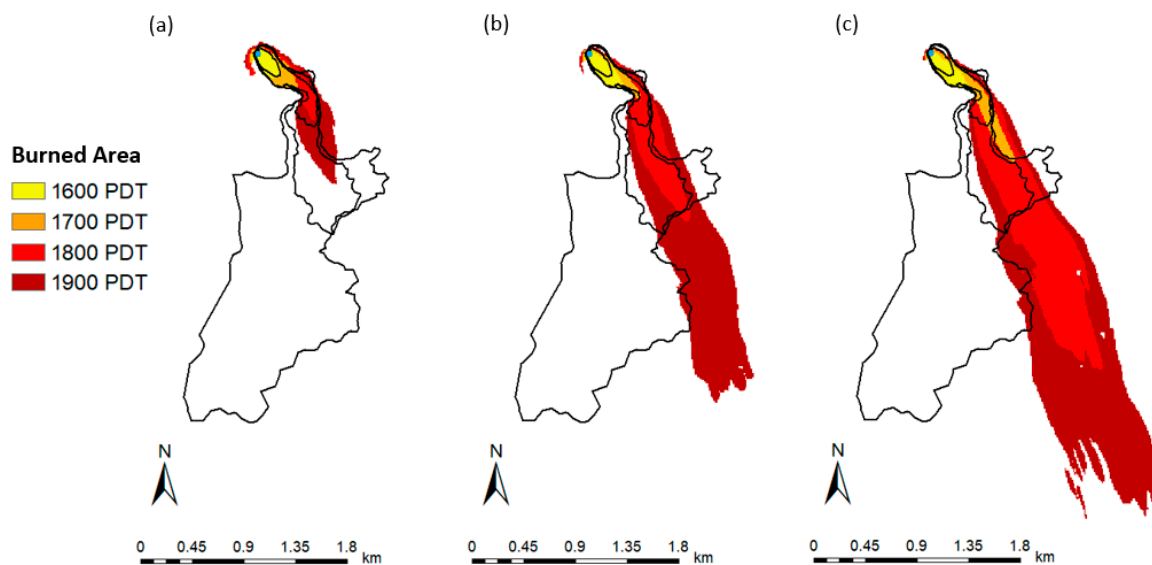


Figure 5. Sherpa fire ignition (blue dot), observed perimeters at 1600, 1700, 1800, and 1900 PDT (black polygons), and the simulated FARSITE burn areas (colored polygons) for simulations with (a) 1.0 GF, (b) 1.4 GF, and (c) 1.7 GF.

Table 3. Specifications for both wildfire case study simulations.

| | | |
|--------------------------|---------------------------------|------------------------|
| | Distance Resolution | 30 m |
| | Perimeter Resolution | 30 m |
| | Time Step | 10 min |
| <i>Fuel Properties</i> | Canopy Cover | 10% |
| | Stand Height | 3 m |
| | Base Stand Height | 0.1 m |
| | Canopy Bulk Density | 0.2 kg m ⁻³ |
| | Foliar Moisture Content | 50% |
| <i>Spotting Settings</i> | Spot Probability | 5 % |
| | Spot Delay | 0 min |
| | Min. Spot Distance | 12 m |
| | Background Spot Grid Resolution | 6 m |

Table 4. Quantitative metrics for the Sherpa (top) and Painted Cave (bottom) simulations. The simulation with the burned area closest to observed and the highest SM value at each time is in bold. The all-FM1 simulation was assessed separately.

| SHERPA | Burned Area (ha) | | | | SM | | | |
|---------------------|------------------|-------------|-------------|--------------|-------------|-------------|-------------|-------------|
| | 1600 | 1700 | 1800 | 1900 | 1600 | 1700 | 1800 | 1900 |
| Observed Perimeters | 3.0 | 11.8 | 46.6 | 246.6 | - | - | - | - |
| 1.0 GF | 3.8 | 8.0 | 13.8 | 33.0 | 0.84 | 0.66 | 0.37 | 0.17 |
| 1.4 GF | 5.1 | 8.2 | 32.9 | 128.6 | 0.64 | 0.68 | 0.64 | 0.25 |
| 1.7 GF | 5.2 | 14.3 | 95.2 | 237.5 | 0.57 | 0.68 | 0.40 | 0.21 |

| PAINTED CAVE | Burned Area (ha) | | | | SM | | | |
|--------------------|------------------|--------------|--------------|--------------|-------------|-------------|-------------|-------------|
| | 1900 | 2000 | 2100 | 2200 | 1900 | 2000 | 2100 | 2200 |
| Observed Perimeter | 1792 (final) | 1792 (final) | 1792 (final) | 1792 (final) | - | - | - | - |
| 1.0 GF | 37 | 153 | 296 | 407 | 0.05 | 0.16 | 0.28 | 0.37 |
| 1.4 GF | 43 | 162 | 265 | 351 | 0.04 | 0.17 | 0.26 | 0.33 |
| 1.7 GF | 64 | 195 | 298 | 380 | 0.07 | 0.20 | 0.29 | 0.36 |
| 2.0 GF | 95 | 210 | 247 | 256 | 0.10 | 0.21 | 0.24 | 0.25 |
| 1.7 GF—all FM1 | 156 | 587 | 1097 | 1720 | 0.16 | 0.49 | 0.71 | 0.76 |

It should be noted that the observed fire spread further west than the simulated perimeters at 1800 and 1900 PDT due to firefighting efforts limiting the eastward spread toward populated regions [40]. It is possible, however, that local wind shifts and/or terrain effects may have contributed to the observed westward spread, although these were not evident in observations (from RHWC1), WRF, or WN. Additional simulations were performed in which “barriers” (unburnable areas) were applied to limit the eastward spread (not shown). Nevertheless, strong northwesterly winds drove the fire into the barriers and caused the simulated fire to extinguish rather than change direction.

We examined FARSITE sensitivity to initial conditions by running additional simulations with ignitions at 1300, 1400, 1600, and 1700 PDT, and applying a 1.7 GF (see Appendix A). Including the original simulation with an ignition time at 1500 PDT, the five simulations ranged in southward extents three and four hours after ignition, where ignitions with later start times spread further south due to the presence of stronger northerly winds later in the evening (Figure A1a,b). The sensitivity to ignition location was analyzed by running simulations with ignition sites approximately ½ km to the west, southwest, southeast, and east of the original ignition location. Simulations with the west and southwest ignition sites did not spread as far south as the east and southeast ignition sites because of the unburnable region to the south, which limited potential simulated fire spread (Figure A1c,d). As expected, we observed differences in simulated fire spread perimeters when the ignition time or location varied. Nonetheless, there was less agreement between simulations when ignition time varied because of the temporal wind variability. These sensitivity tests demonstrate how relatively small changes in model input can affect FARSITE perimeter accuracy.

3.2. Painted Cave Fire

Simulations for the Painted Cave Fire started at 1800 PDT, and all perimeters were compared to the one, final perimeter and firefighter recollections (see Case Studies Section) to examine southward spread. FARSITE parameterizations were the same as the Sherpa Fire (Table 3). The simulations using the fuel map (Figure 2c) and GF values of 1.0, 1.4, and 1.7 produced perimeters that significantly underestimated firefighter observations. As previously stated, the observed fire reached San Antonio Creek Rd (~3 km) 20 min after ignition; however, it took over 3 h to reach this location in the simulations (Figure A2). In an attempt to simulate faster fire spread, we applied a new fuel map with different chaparral fuels (Figure 6). The new fuel models (FM), FM145 and FM147 [52], replaced FMs 15 and 16 [53], respectively, and were most prominent in the region south of the ignition point (Table 2). The original FMs have produced smaller perimeters compared to the use of Anderson’s fuel models [41]

from lower fuel loadings [77], and the new fuel map should produce larger simulated perimeters and faster fire spread.

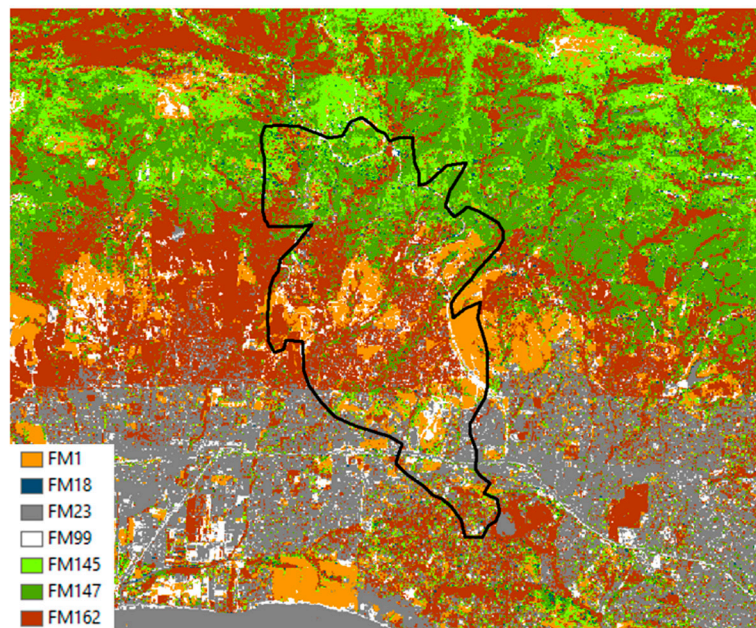


Figure 6. New fuel map for the Painted Cave fire, incorporating FM145 and FM147.

Simulations were performed using GFs of 1.0, 1.4, and 1.7 (Figure 7), and the burned area and SM at each time step during each GF simulation are shown in Table 4. As expected, the perimeters spread south more rapidly using the new fuel map, especially one and two hours after ignition. However, the fire still did not reach San Antonio Creek Rd until three hours after ignition in the 1.7 GF simulation (Figure 7c). Nonetheless, the simulated fire reached the road within two hours when a 2.0 GF was utilized (Figure 7d). Regardless of the GF, all simulations vastly underestimated the time to reach San Antonio Creek Rd, and no simulations reached Highway 101 even after four hours. Furthermore, all simulations stopped around the same location after four hours, even though there were burnable fuels downwind of the fire front. Similar to the Sherpa Fire, we examined the sensitivity to varied fire ignition time and location (see Appendix A). These simulations produced marginally different fire spread perimeters, and all significantly underestimated the observed perimeter (Figure A3).

Finney (1998) suggested that FARSITE can produce reasonable fire perimeters with proper judgement and adjustments [78]. In an attempt to simulate very rapid spread during the Painted Cave Fire, we developed an additional FARSITE sensitivity test with an all-grass (FM1) fuel map and a 1.7 GF, retaining all other inputs and parameterizations. Albeit a homogeneous fuel map is unrealistic for this region, the simulated fire spread significantly further and grew more laterally than the original run (Figure 8a). The simulation reached San Antonio Creek Rd within the first two hours and Highway 101 within the first four hours. Three and four hours after ignition, the simulated areas burned were 1097 and 1720 ha and the SM values (compared to the final perimeter) were 0.71 and 0.76, respectively.

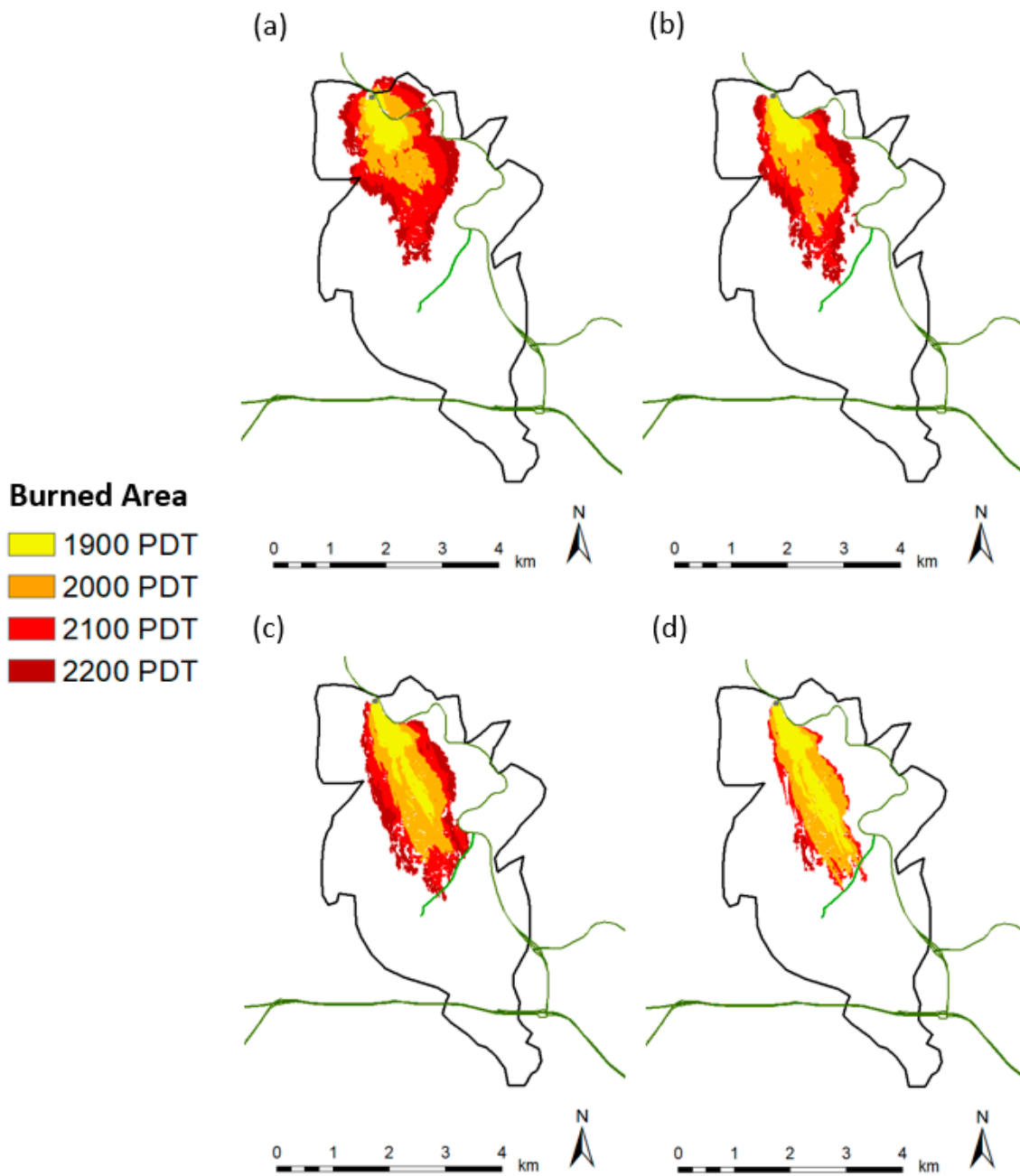


Figure 7. Painted Cave fire ignition site (light grey dot), official fire perimeter (black polygon), and simulated burn areas (colored polygons) for (a) GF 1.0, (b) GF 1.4, (c) GF 1.7, and (d) GF 2.0. The green lines indicate important reference roads; the dark green line in the southern part of the fire perimeter is Highway 101, the dark green line in the eastern part of the fire perimeter is Highway 154, and the light green line in the middle of the perimeter is San Antonio Creek Rd.

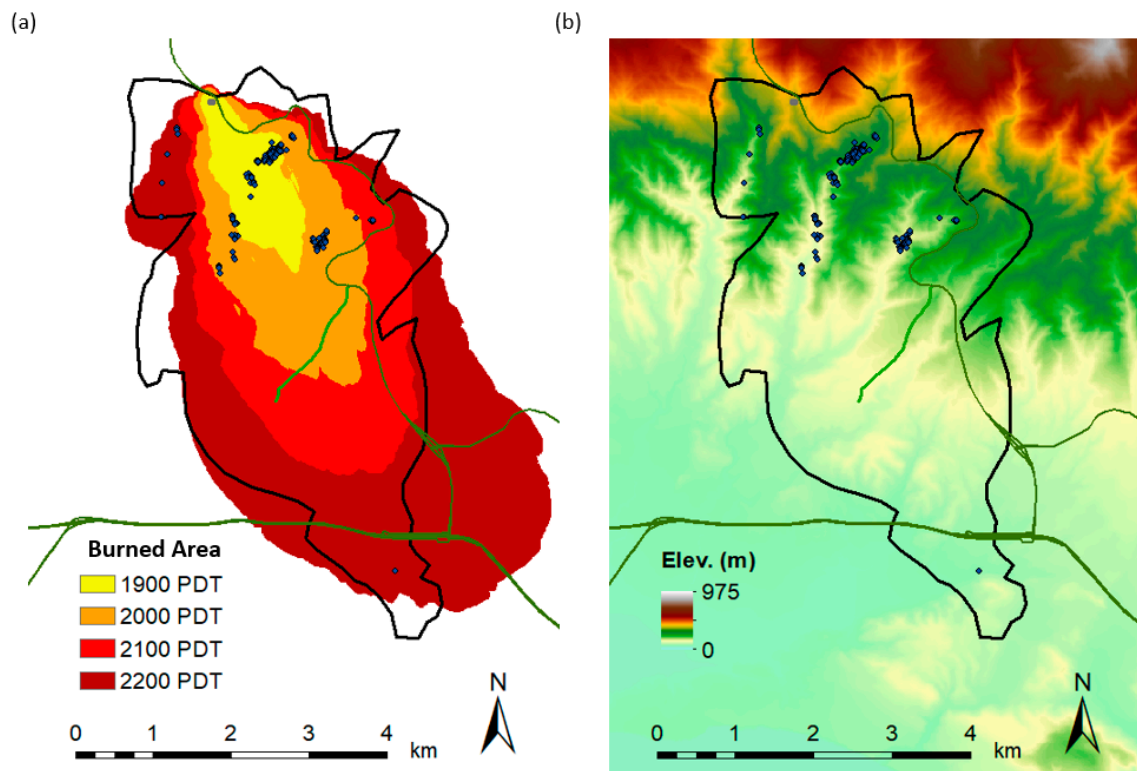


Figure 8. (a) Similar to Figure 7, except the simulated burn areas (colored polygons) are from the all-grass fuel map simulation. Blue dots indicate ember launch locations for spot fires. (b) Same as (a) with elevation colored.

3.3. Spotting Limitations

Understanding spotting is crucial for realistically simulating wildfires in this region, and in many other mountain areas with similar fire weather regimes. Firefighters recall the significant amount of spotting that resulted in the rapid, downslope spread of the Painted Cave fire [40]. However, in our simulations, FARSITE produced spotting only in valleys towards uphill slopes (to the south), shown in Figure 8b. Thus, if spotting was a major factor for the observed rapid spread of this fire, limitations in simulating spotting locations likely led to large underestimations in fire spread, regardless of fuel model or wind speed.

To analyze spotting in FARSITE using a simple simulation, we created east-west oriented ridges and valleys with 10° , 20° , and 30° slopes. Simulations were performed using a constant fuel model (FM15) and wind (13.41 m/s from 315°) over the entire domain with a 5% spot probability (same as all previous simulations). Figure 9 shows ember launch and landing locations for these simulations. The ridge and valley simulations with slopes less than 10° produced little to no spotting. In simulations with steeper slopes, the ember launch site was always lower in elevation than the landing site, and this was consistent with spotting patterns in the Sherpa and Painted Cave fire simulations (Figure 8). As expected by the spotting equations used in FARSITE [43], embers landed in the direction the wind was blowing (southeast in the idealized case). One potential explanation for the lack of upslope-landing embers is that embers were launched during downslope fire spread, but extinguished mid-air from the loss of density and volume during burning [27]. Another limitation of FARSITE is that only horizontal winds are simulated, precluding a more realistic three-dimensional structure of turbulence in spotting parameterizations. Furthermore, embers are not launched in simulated backing fires due to lower intensities [27], which may contribute to the lack of spotting during our downslope fire spread. To summarize, spotting and the overall simulated wildfire spread during fires driven by strong downslope

winds is limited by the inability of landing embers downslope and thresholds for maximum distance or time before ember burnout in FARSITE.

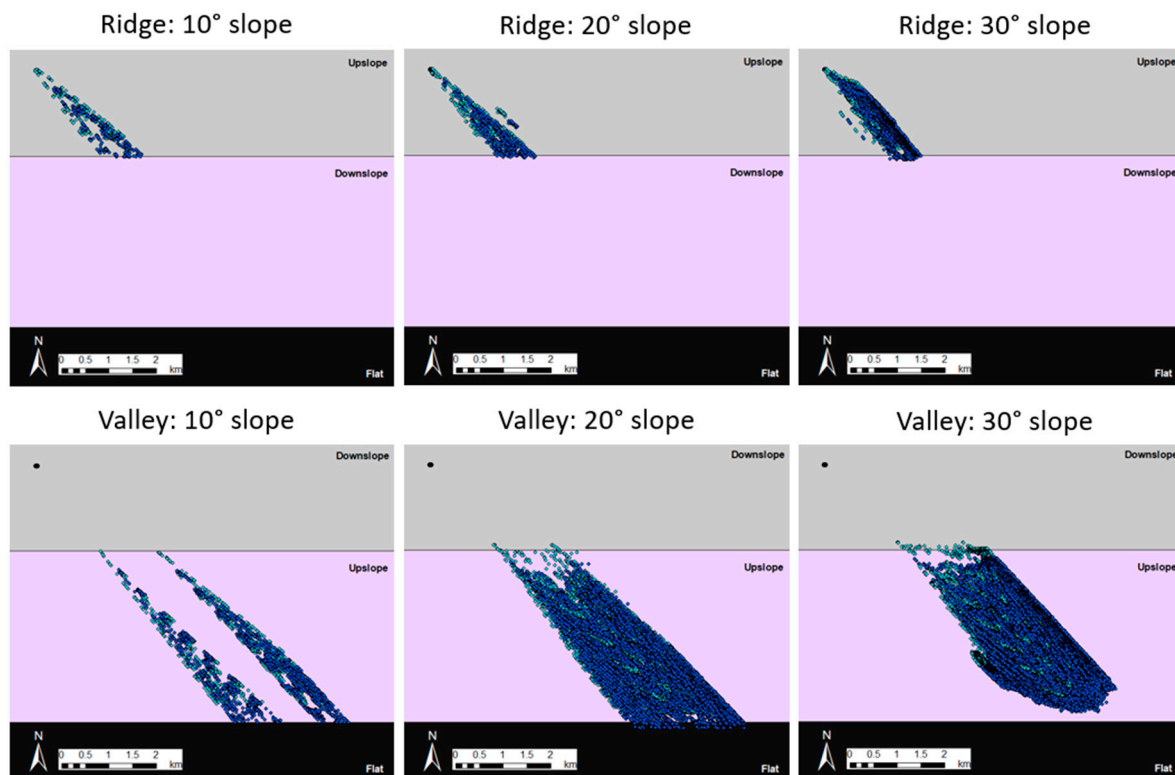


Figure 9. Spotting launch (light blue) and land (dark blue) locations on an idealized east-west oriented ridge (top) or valley (bottom) with differing slopes from the same ignition point (black dot in upper-left corner). Constant 13.41 m/s (30 mph) NW (315°) winds were applied. The fuel map used was all FM15 (chamise), although results are consistent with other fuel models tested such as FM1 (grass) and FM16 (ceanothus).

3.4. FlamMap Comparisons

FlamMap MTT simulations were completed for the Sherpa and Painted Cave fires to examine whether FlamMap has the potential to produce more accurate fire perimeters than FARSITE when compared to the observed perimeters. As explained in the Introduction, FlamMap and FARSITE are similar in that they use the same surface fire, crown fire, and spotting models. Therefore, the spotting limitations found in FARSITE were also present in FlamMap.

The main difference between the two models is the inability for FlamMap to use temporally-variable gridded winds. To properly compare simulations between FlamMap and FARSITE, both models were run using only the WN raster at the respective ignition times with a 1.7 GF. The Sherpa Fire simulations in both FARSITE and FlamMap underestimated the actual area burned by the fire (Figure A4), primarily because winds later in the evening were stronger than those at the time of ignition, and the simulated fire was run into the unburnable area south of the ignition point, thus extinguishing. This finding highlights the importance of simulating wildfires with models that allow for spatially and temporally variable wind input during extreme winds, although the simulated fire was underestimated in both FARSITE and FlamMap potentially from underestimated wind input.

Figure 10 shows the observed Painted Cave Fire perimeter and the FARSITE and FlamMap local time perimeters. While FlamMap underestimated southward spread compared to the observed perimeter, it simulated fire spread further south and laterally. Interestingly, FlamMap and FARSITE produced similar perimeters in the first hour after ignition, but FlamMap spread more west, south,

and east in all subsequent hours. The simulated fires grew to approximately the same southward point, near San Antonio Creek Rd, before significantly slowing spread. Upon investigation, WN produced slower winds in this region that likely decelerated southward fire spread. The differences shown in Figure 10 likely result from inherent differences in the model’s equations; FARSITE uses Huygen’s wave propagation principle to simulate wildfire spread, whereas FlamMap MTT calculates fire behavior at each grid cell individually [32]. Importantly, the same spotting limitations were evident in both models, which led to the significant underestimation in spread during the Painted Cave Fire. This is essential to understand when applying these models in operational settings for emergency management and evacuation planning, particularly in regions with complex terrain and downslope of mountains.

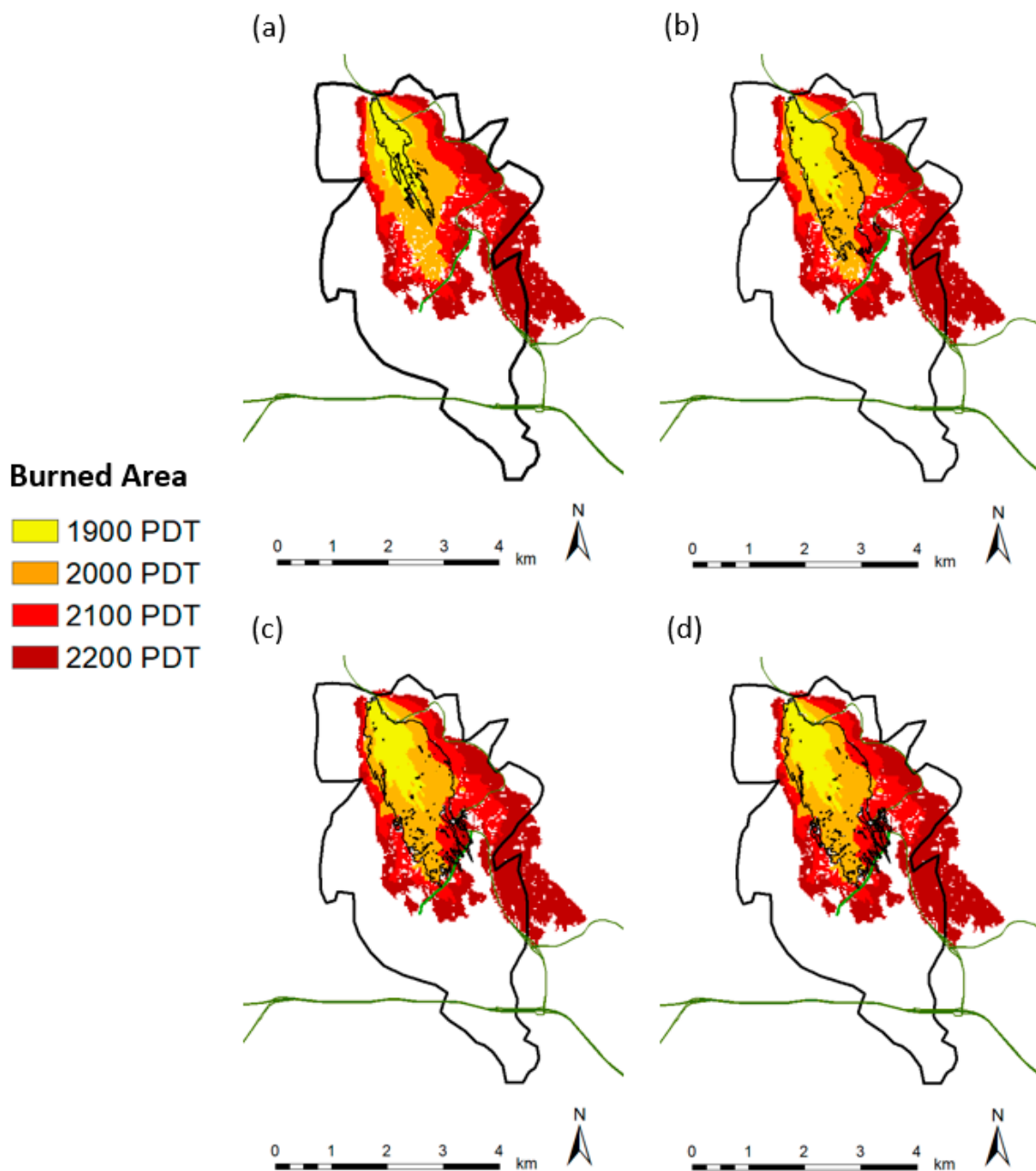


Figure 10. Same as Figure 7 with the FlamMap and FARSITE burn areas (thin, black polygons) at (a) 1900, (b) 2000, (c) 2100, and (d) 2200 PDT.

4. Conclusions

This study investigates the performance of FARSITE in simulating rapidly spreading wildfires on the southern slopes of the SYM in coastal Santa Barbara. Understanding wildfire risk is especially important in the wildland-urban interface in areas such as coastal Santa Barbara, where advances in evacuation planning and emergency management preparedness will increase resilience to these natural hazards. This study is also applicable to other regions where downslope windstorms are frequent. Two case studies in coastal Santa Barbara County were selected to simulate wildfires significantly influenced by extreme fire weather conditions associated with downslope winds known as Sundowners. The 2016 Sherpa Fire and the 1990 Painted Cave Fire were simulated using FARSITE by downscaling 1 km WRF output run to 100 m resolution using WN. In Sherpa Fire simulations, perimeters were generally underestimated with a 1.0 and 1.4 GF applied to WN rasters, and overestimated with a 1.7 GF except for the 1900 PDT perimeter, which underestimated the area burned by less than 10 ha. In all cases, the final simulated burned areas did not reproduce the substantial southwestward growth of the actual fire. This exposes the inability of the SM to account for directional differences of the burned areas under examination. In general, utilizing a wind downscaling software and applying a gust factor produced more accurate fire perimeters for the Sherpa Fire.

In contrast, all simulated Painted Cave Fire perimeters were underestimated, including the all-grass fuel map simulation which produced the fastest fire spread. We hypothesize that these discrepancies can be largely explained by enhanced spotting during this event, visually documented by fire fighters. The wind inputs to FARSITE and FlamMap are two-dimensional. Consequently, the simulations are unable to track embers lofted into terrain following wind fields which would likely land downslope more quickly than the simulations allow. Understanding the spotting limitations found here in FARSITE and FlamMap is exceedingly important for operational purposes, especially for wildfires in complex terrain or during downslope fire spread. Another factor that may have caused the underestimated growth rate is the algorithm the fire model uses to assimilate the fuel characteristics of the various dead and live components, especially the different sizes. A concurrent study currently in publication review suggests that maintaining the size characteristics of the fine fuels may enhance the simulated spread rates [79].

FARSITE has the potential to provide reliable perimeters for simulating wildfires in Santa Barbara influenced by Sundowner winds, although it may not capture extreme cases with large amounts of spotting downslope of the mountains. Future work should be carried out to estimate the spatiotemporal variability of the gust factor during Sundowner events and apply a methodology to gridded wind data for use in wildfire modeling. This would be particularly important in regions with complex terrain and highly variable wind and gust patterns. The authors believe inherent limitations in FARSITE are preventing downslope spotting and thus underestimating simulated fire perimeters in cases with a significant amount of spotting. This problem may be solved by examination and improvement of the spotting algorithm in the software. Additionally, FARSITE can be useful for wildfires spreading upslope, or in cases where downslope winds are not the dominant variable controlling fire spread, although this requires further testing. Advancing knowledge on weather and fire modeling in coastal Santa Barbara will increase resilience and allow for improved fire risk management and city planning.

Author Contributions: Conceptualization, K.Z., L.M.V.C., S.P., F.F., G.-J.D., C.J., D.R. and M.M.; methodology, K.Z., L.M.V.C., S.P., F.F., G.-J.D., C.J. and D.R.; formal analysis, K.Z.; data curation, K.Z., S.P., G.-J.D. and C.J.; writing—original draft preparation, K.Z.; writing—review and editing, K.Z., L.M.V.C., S.P., F.F., G.-J.D., C.J., D.R. and M.M.; visualization, K.Z.; supervision, L.M.V.C.; project administration, K.Z. and L.M.V.C.; funding acquisition, L.M.V.C., S.P., F.F., C.J., D.R. and M.M. All authors have read and agreed to the published version of the manuscript.

Funding: This research was supported by the NSF-PREEVENTS ICER—1664173.

Acknowledgments: This research was completed with the help of the National Weather Service – Los Angeles/Oxnard Office and the Montecito, Santa Barbara, and Santa Barbara County Fire Departments. Discussions on the evolution of wildfire perimeters with Chief Rob Hazard (Santa Barbara County Fire Department) and with

John Benoit on FARSITE were much appreciated. The authors acknowledge the National Center for Atmospheric Research, Computational and Information Systems Laboratory, Boulder, CO.

Conflicts of Interest: The authors declare no conflict of interest.

Appendix A

Table A1. Descriptions of all abbreviations used in the manuscript.

| ABBREVIATION | DESCRIPTION |
|--------------|--|
| FARSITE | Fire Area Simulator |
| FM | Fuel model |
| GF | Gust factor |
| KSBA | Santa Barbara Airport weather station |
| MTT | Minimum Travel Time |
| RAWS | Remote Automatic Weather Station |
| RHWC1 | Refugio weather station |
| SM | Sorensen Metric |
| SYM | Santa Ynez Mountains |
| WN | WindNinja |
| WRF | Weather Research and Forecasting model |

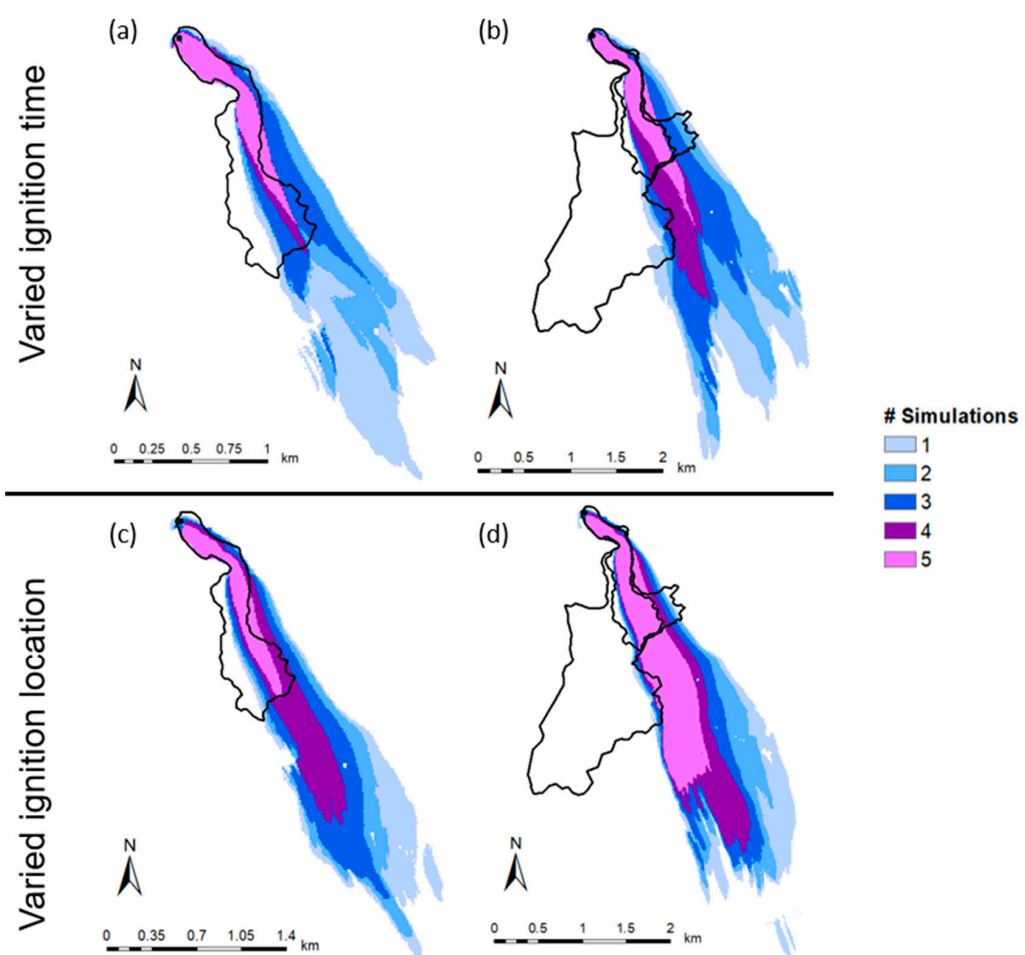


Figure A1. (a) Sherpa fire ignition site (black dot), observed perimeters (black contours) at 1800 PDT, and the count of overlapping simulations three hours after ignition in the varied ignition time simulations. (b) Same as (a) with the 1900 PDT observed perimeter added and the count of overlapping simulations four hours after ignition. (c) same as (a) with the count of overlapping simulations in the varied location simulations three hours after ignition. (d) same as (c) four hours after ignition.

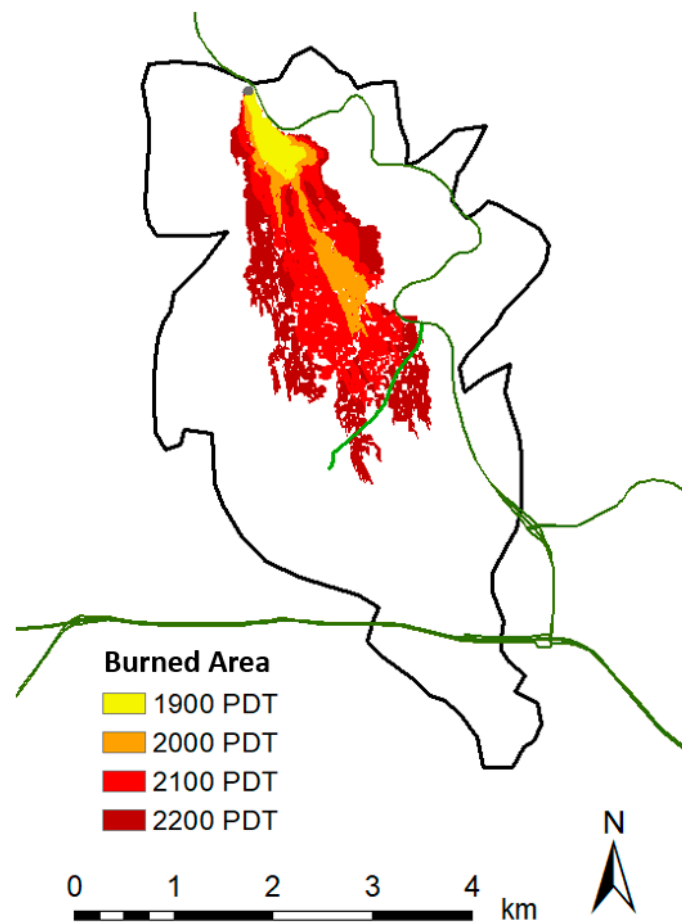


Figure A2. Same as Figure 7c using the original fuel map (shown in Figure 2c).

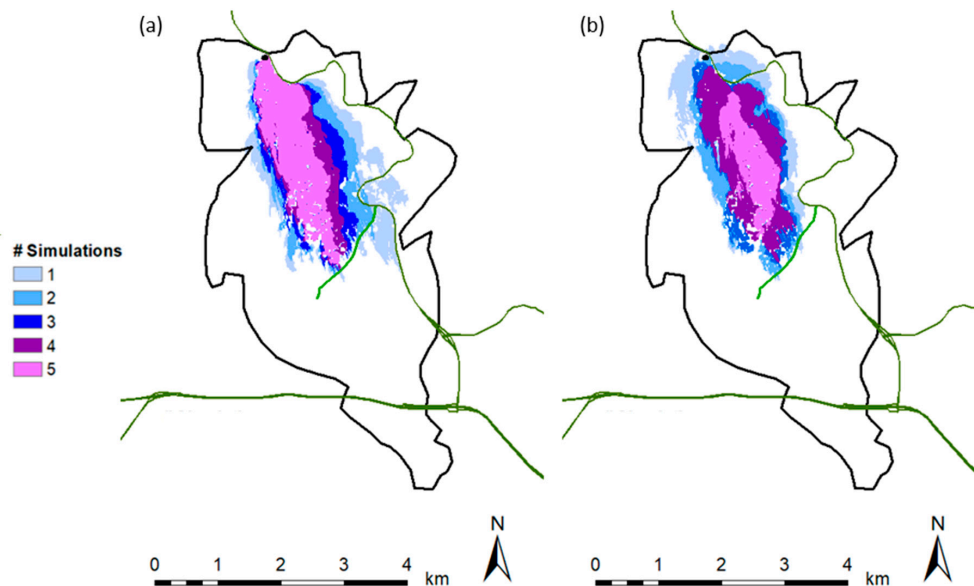


Figure A3. Painted Cave fire perimeter and reference roads (see Figure 7 for details). Colored polygons in (a) are the count of simulations four hours after ignition in the varied ignition time simulations. (b) The count of simulations four hours after ignition using varied ignition locations.

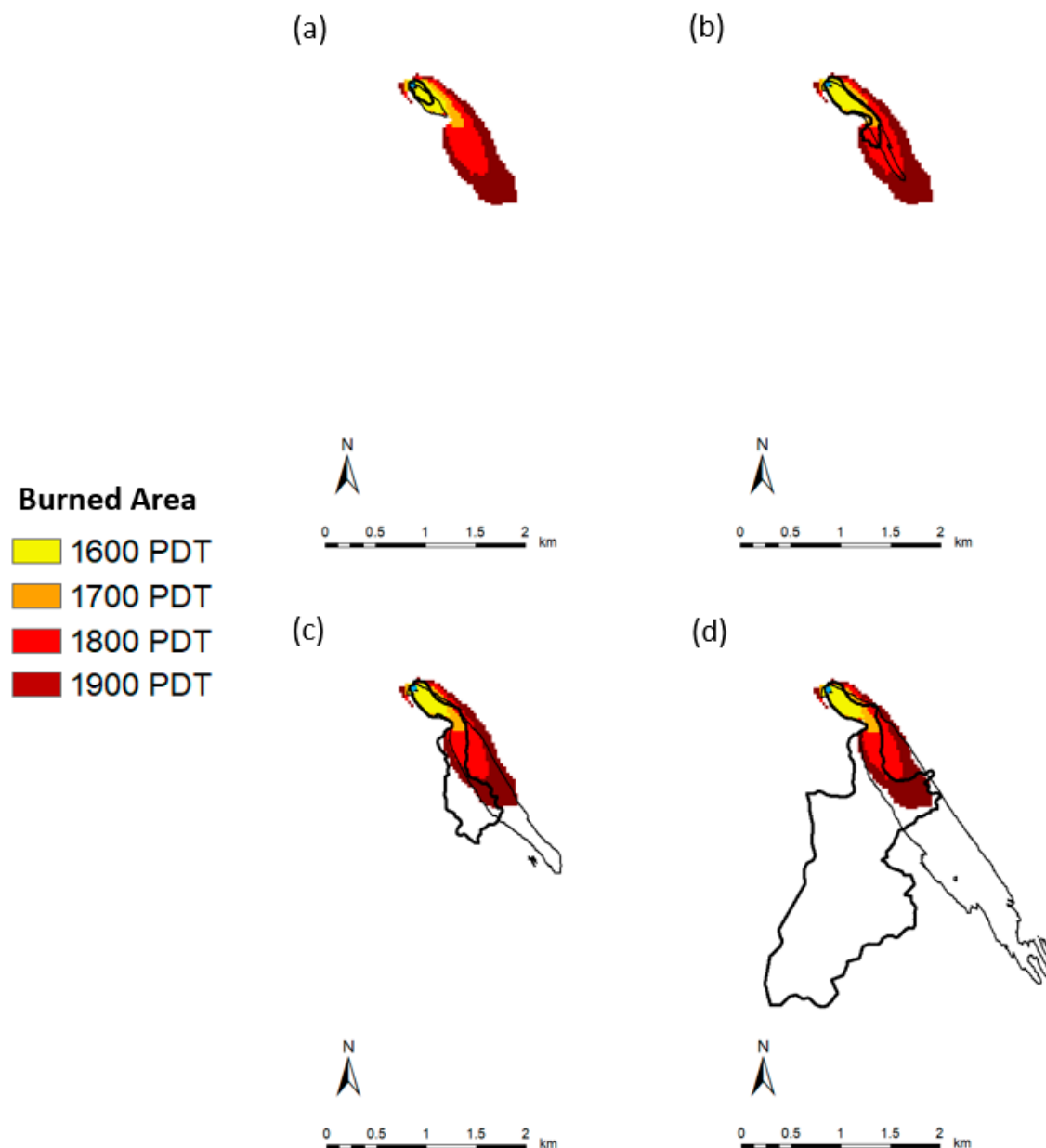


Figure A4. Sherpa fire perimeters with FlamMap local time burnt areas (colored polygons), FARSITE perimeters (thin black polygons), and observed perimeters (thick black polygons) at (a) 1600 PDT, (b) 1700 PDT, (c) 1800 PDT, and (d) 1900 PDT.

References

1. Richardson, L.A.; Champ, P.A.; Loomis, J.B. The Hidden Cost of Wildfires: Economic Valuation of Health Effects of Wildfire Smoke Exposure in Southern California. *JFE* **2012**, *18*, 14–35. [[CrossRef](#)]
2. Parise, M.; Cannon, S.H. Wildfire Impacts on the Processes That Generate Debris Flows in Burned Watersheds. *Nat. Hazards* **2012**, *61*, 217–227. [[CrossRef](#)]
3. Westerling, A.L.; Hidalgo, H.G.; Cayan, D.R.; Swetnam, T.W. Warming and Earlier Spring Increase Western U.S. Forest Wildfire Activity. *Science* **2006**, *313*, 940–943. [[CrossRef](#)] [[PubMed](#)]
4. Diffenbaugh, N.S.; Swain, D.L.; Touma, D. Anthropogenic Warming Has Increased Drought Risk in California. *Proc. Natl. Acad. Sci. USA* **2015**, *112*, 3931–3936. [[CrossRef](#)]
5. Abatzoglou, J.T.; Williams, A.P. Impact of Anthropogenic Climate Change on Wildfire across Western US Forests. *Proc. Natl. Acad. Sci. USA* **2016**, *113*, 11770–11775. [[CrossRef](#)]

6. Cayan, D.R.; Maurer, E.P.; Dettinger, M.D.; Tyree, M.; Hayhoe, K. Climate Change Scenarios for the California Region. *Clim. Chang.* **2008**, *87* (Suppl. 1), 21–42. [[CrossRef](#)]
7. Syphard, A.D.; Clarke, K.C.; Franklin, J. Simulating Fire Frequency and Urban Growth in Southern California Coastal Shrublands, USA. *Landsc. Ecol.* **2007**, *22*, 431–445. [[CrossRef](#)]
8. Syphard, A.D.; Radeloff, V.C.; Keuler, N.S.; Taylor, R.S.; Hawbaker, T.J.; Stewart, S.I.; Clayton, M.K. Predicting Spatial Patterns of Fire on a Southern California Landscape. *Int. J. Wildland Fire* **2008**, *17*, 602. [[CrossRef](#)]
9. Faivre, N.; Jin, Y.; Goulden, M.L.; Randerson, J.T. Controls on the Spatial Pattern of Wildfire Ignitions in Southern California. *Int. J. Wildland Fire* **2014**, *23*, 799. [[CrossRef](#)]
10. Syphard, A.D.; Keeley, J.E. Location, Timing and Extent of Wildfire Vary by Cause of Ignition. *Int. J. Wildland Fire* **2015**, *24*, 37. [[CrossRef](#)]
11. Countryman, C.M. *The Fire Environment Concept*; USDA Forest Service: Berkeley, CA, USA, 1972; p. 15.
12. Rothermel, R.C. *A Mathematical Model. for Predicting Fire Spread in Wildland Fuels*; Research Paper INT-115; U.S. Department of Agriculture, Forest Service, Intermountain Forest and Range Experiment Station: Ogden, UT, USA, 1972; p. 40.
13. Rothermel, R.C. *How to Predict the Spread and Intensity of Forest and Range Fires*; Research Paper INT-GTR-143; U.S. Department of Agriculture, Forest Service, Intermountain Forest and Range Experiment Station: Ogden, UT, USA, 1983.
14. Catchpole, W.; Bradstock, R.; Choate, J.; Fogarty, L.; Gellie, N.; McCarthy, G.; McCaw, W.; Marsden-Smedley, J.; Pearce, G. Co-operative Development of Equations for Heathland Fire Behaviour. In Proceedings of the 3rd International Conference of Forest Fire Research, Luso, Portugal, 16–20 November 1998.
15. Moritz, M.A. Spatiotemporal Analysis of Controls on Shrubland Fire Regimes: Age Dependency and Fire Hazard. *Ecology* **2003**, *84*, 351–361. [[CrossRef](#)]
16. Keeley, J.E.; Safford, H.; Fotheringham, C.J.; Franklin, J.; Moritz, M. The 2007 southern California wildfires: Lessons in complexity. *J. For.* **2009**, *107*, 287–296.
17. Stratton, R.D. *Guidebook on LANDFIRE Fuels Data Acquisition, Critique, Modification, Maintenance, and Model Calibration*; Technical Report Np. RMRS-GTR-220; U.S. Department of Agriculture, Forest Service, Rocky Mountain Research Station: Fort Collins, CO, USA, 2009; pp. 1–54.
18. Moritz, M.A.; Moody, T.J.; Krawchuk, M.A.; Hughes, M.; Hall, A. Spatial Variation in Extreme Winds Predicts Large Wildfire Locations in Chaparral Ecosystems: Extreme Winds and Large Wildfires. *Geophys. Res. Lett.* **2010**, *37*. [[CrossRef](#)]
19. Ryan, G. *Downslope Winds of Santa Barbara, California*; NOAA Technical Memorandum NWS WR-240; Scientific Services Division, Western Region: Salt Lake City, UT, USA, 1996.
20. Blier, W. The Sundowner Winds of Santa Barbara, California. *Weather Forecast.* **1998**, *13*, 702–716. [[CrossRef](#)]
21. Hatchett, B.J.; Smith, C.M.; Nauslar, N.J.; Kaplan, M.L. Brief Communication: Synoptic-Scale Differences between Sundowner and Santa Ana Wind Regimes in the Santa Ynez Mountains, California. *Nat. Hazards Earth Syst. Sci.* **2018**, *18*, 419–427. [[CrossRef](#)]
22. Smith, C.M.; Hatchett, B.J.; Kaplan, M.L. Characteristics of Sundowner Winds near Santa Barbara, California, from a Dynamically Downscaled Climatology: Environment and Effects near the Surface. *J. Appl. Meteor. Climatol.* **2018**, *57*, 589–606. [[CrossRef](#)]
23. Sukup, S. *Extreme Northeasterly Wind Events in the Hills above Montecito, California*; Western Region Technical Attachment NWS WR-1302; NWS Western Region: Salt Lake City, UT, USA, 2013; p. 21.
24. Cannon, F.; Carvalho, L.M.V.; Jones, C.; Hall, T.; Gomberg, D.; Dumas, J.; Jackson, M. WRF Simulation of Downslope Wind Events in Coastal Santa Barbara County. *Atmos. Res.* **2017**, *191*, 57–73. [[CrossRef](#)]
25. Murray, A.T.; Carvalho, L.; Church, R.L.; Jones, C.; Roberts, D.A.; Xu, J.; Zigner, K.; Nash, D. Coastal vulnerability under extreme weather. In *Applied Spatial Analysis and Policy Special Issue: Contemporary Applications for Spatially Integrated Social Science*; Springer: New York, NY, USA, (under review).
26. Peterson, S.H. Fire Risk in California. Ph.D. Thesis, University of California, Santa Barbara, CA, USA, 2011.
27. Finney, M.A. *FARSITE: Fire Area Simulator-Model Development and Evaluation*; Research Paper RMRS-RP-4; U.S. Department of Agriculture, Forest Service, Rocky Mountain Research Station: Fort Collins, CO, USA, 1998.
28. Finney, M.A.; Bradshaw, L.; Butler, B.W. *Modeling Surface Winds in Complex Terrain for Wildland Fire Incident Support*; Final Report for JFSP Funded Project #03-2-1-04; U.S. Department of Agriculture, Forest Service: Fort Collins, CO, USA, 2006; pp. 1–10.

29. Stratton, R.D. *Guidance on Spatial Wildland Fire Analysis: Models, Tools, and Techniques*; General Technical Report RMRS-GTR-183; U.S. Department of Agriculture, Forest Service, Rocky Mountain Research Station: Ft. Collins, CO, USA, 2006. [[CrossRef](#)]
30. Finney, M.A.; Ryan, K.C. Use of the FARSITE Fire Growth Model for Fire Prediction in U.S. National Parks. In Proceedings of the International Emergency Management and Engineering Conference, San Diego, CA, USA, 9–12 May 1995; pp. 183–189.
31. Arca, B.; Duce, P.; Laconi, M.; Pellizzaro, G.; Salis, M.; Spano, D. Evaluation of FARSITE Simulator in Mediterranean Maquis. *Int. J. Wildland Fire* **2007**, *16*, 563. [[CrossRef](#)]
32. Papadopoulos, G.D.; Pavlidou, F.-N. A Comparative Review on Wildfire Simulators. *IEEE Syst. J.* **2011**, *5*, 233–243. [[CrossRef](#)]
33. Phillips, D.R.; Waldrop, T.A.; Simon, D.M. Assessment of the FARSTE model for predicting fire behavior in the Southern Appalachian Mountains. General Technical Report SRS-92. In *Proceedings of the 13th Biennial Southern Silvicultural Research Conference*; U.S. Department of Agriculture, Forest Service: Asheville, NC, USA, 2006; pp. 521–525.
34. Forghani, A.; Cechet, B.; Radke, J.; Finney, M.; Butler, B. Applying Fire Spread Simulation over Two Study Sites in California Lessons Learned and Future Plans. In Proceedings of the 2007 IEEE International Geoscience and Remote Sensing Symposium, Barcelona, Spain, 23–28 July 2007; pp. 3008–3013. [[CrossRef](#)]
35. Scott, J.H. *Comparison of Crown Fire Modeling Systems Used in Three Fire Management Applications*; RMRS-RP-58; U.S. Department of Agriculture, Forest Service, Rocky Mountain Research Station: Ft. Collins, CO, USA, 2006. [[CrossRef](#)]
36. Coen, J.L.; Cameron, M.; Michalakes, J.; Patton, E.G.; Riggan, P.J.; Yedinak, K.M. WRF-Fire: Coupled Weather–Wildland Fire Modeling with the Weather Research and Forecasting Model. *J. Appl. Meteor. Climatol.* **2013**, *52*, 16–38. [[CrossRef](#)]
37. Skamarock, W.C.; Klemp, J.B. A Time-Split Nonhydrostatic Atmospheric Model for Weather Research and Forecasting Applications. *J. Comput. Phys.* **2008**, *227*, 3465–3485. [[CrossRef](#)]
38. Kochanski, A.K.; Jenkins, M.A.; Mandel, J.; Beezley, J.D.; Krueger, S.K. Real Time Simulation of 2007 Santa Ana Fires. *For. Ecol. Manag.* **2013**, *294*, 136–149. [[CrossRef](#)]
39. Gollner, M.; Trouv'e, A.; Altintas, I.; Block, J.; De Callafon, R.; Clements, C.; Cortes, A.; Ellicott, E.; Filippi, J.B.; Finney, M.; et al. Towards data-driven operational wildfire spread modeling. In *Report of the NSF-Funded Wildfire Workshop*; University of Maryland: College Park, MD, USA, 2015.
40. Hazard, R.; Chief of Santa Barbara County Fire Department, Santa Barbara, CA, USA. Personal communication, 2019.
41. Anderson, H.E. *Aids to Determining Fuel Models for Estimating Fire Behavior*; General Technical Report INT-GTR-122; U.S. Department of Agriculture, Forest Service, Intermountain Forest and Range Experiment Station: Ogden, UT, USA, 1982. [[CrossRef](#)]
42. Van Wagner, C.E. Conditions for the start and spread of crown fire. *Can. J. For. Res.* **1977**, *7*, 23–34. [[CrossRef](#)]
43. Albini, F.A. *Spot Fire Distance from Burning Trees: A Predictive Model*; Intermountain Forest and Range Experiment Station, Forest Service, U.S. Department of Agriculture: Ogden, UT, USA, 1979; Volume 56.
44. Andrews, P.L. BehavePlus Fire Modeling System: Past, Present, and Future. In Proceedings of the 7th Symposium on Fire and Forest Meteorological Society, Bar Harbor, ME, USA, 23–25 October 2007.
45. Hanes, T.L. Ecological Studies on Two Closely Related Chaparral Shrubs in Southern California. *Ecol. Monogr.* **1965**, *35*, 213–235. [[CrossRef](#)]
46. Hanes, T.L. The Vegetation Called Chaparral. In Proceedings of the Symposium on Living with the Chaparral, Sierra Club, San Francisco, CA, USA, 30–31 March 1973; pp. 1–5.
47. Rothermel, R.C.; Philpot, C.W. Predicting Changes in Chaparral Flammability. *J. For.* **1973**, *71*, 640–643.
48. Countryman, C.M.; Philpot, C.W. *Physical Characteristics of Chamise as a Wildland Fuel*; Res. Pap. PSW-66; U.S. Department of Agriculture Forest Service: Berkeley, CA, USA, 1970.
49. Meerdink, S.K.; Roberts, D.A.; Roth, K.L.; King, J.Y.; Gader, P.D.; Koltunov, A. Classifying California plant species temporally using airborne hyperspectral imagery. *Remote Sens. Environ.* **2019**, *232*, 111308. [[CrossRef](#)]
50. Roth, K.L.; Dennison, P.E.; Roberts, D.A. Comparing Endmember Selection Techniques for Accurate Mapping of Plant Species and Land Cover Using Imaging Spectrometer Data. *Remote Sens. Environ.* **2012**, *127*, 139–152. [[CrossRef](#)]

51. Peterson, S.H.; Stow, D.A. Using Multiple Image Endmember Spectral Mixture Analysis to Study Chaparral Regrowth in Southern California. *Int. J. Remote Sens.* **2003**, *24*, 4481–4504. [[CrossRef](#)]
52. Scott, J.H.; Burgan, R.E. *Standard Fire Behavior Fuel Models: A Comprehensive Set for Use with Rothermel's Surface Fire Spread Model*; General Technical Report RMRS-GTR-153; U.S. Department of Agriculture, Forest Service, Rocky Mountain Research Station: Ft. Collins, CO, USA, 2005. [[CrossRef](#)]
53. Weise, D.R.; Regelbrugge, J. Recent Chaparral Fuel Modeling Efforts. In *Chaparral Fuel Modeling Workshop*; 1997; pp. 11–12. Available online: <http://web.physics.ucsb.edu/~complex/research/hfire/fuels/refs/weiseregel1997.pdf> (accessed on 9 July 2020).
54. Farr, T.G.; Rosen, P.A.; Caro, E.; Crippen, R.; Duren, R.; Hensley, S.; Kobrick, M.; Paller, M.; Rodriguez, E.; Roth, L.; et al. The Shuttle Radar Topography Mission. *Rev. Geophys.* **2007**, *45*. [[CrossRef](#)]
55. Duine, G.J.; Jones, C.; Carvalho, L.; Fovell, R. Simulating Sundowner Winds in Coastal Santa Barbara: Model Validation and Sensitivity. *Atmosphere* **2019**, *10*, 155. [[CrossRef](#)]
56. Gibson, C.; Gorski, C. FARSITE Weather Streams from the NWS IFPS System. In Proceedings of the 5th Symposium on Fire and Forest Meteorology; 2003; pp. 1–4. Available online: https://gacc.nifc.gov/nwcc/content/products/intelligence/FARSITE_Wx_DataGenerator.pdf (accessed on 9 July 2020).
57. Carvalho, L.; Duine, G.-J.; Jones, C.; Zigner, K.; Clements, C.; Kane, H.; Gore, C.; Bell, G.; Gamelin, B.; Gomborg, D.; et al. The Sundowner Winds Experiment (SWEX) Pilot Study: Understanding Downslope Windstorms in the Santa Ynez Mountains, Santa Barbara, California. *Mon. Wea. Rev.* **2020**, *148*, 1519–1539. [[CrossRef](#)]
58. Butler, B.W.; Forthofer, J.M. *Gridded Wind Data: What Is It and How Is It Used? Report on file*; U.S. Department of Agriculture, Forest Service, Rocky Mountain Research Station, Fire Sciences Lab.: Missoula, MT, USA, 2004.
59. Salis, M. Fire Behavior Simulation in Mediterranean Marquis using FARSITE. Ph.D. Thesis, University of Sassari, Sassari, Italy, 2008.
60. Forthofer, J.M.; Butler, B.W.; Wagenbrenner, N.S. A Comparison of Three Approaches for Simulating Fine-Scale Surface Winds in Support of Wildland Fire Management. Part I. Model Formulation and Comparison against Measurements. *Int. J. Wildland Fire* **2014**, *23*, 969. [[CrossRef](#)]
61. Forthofer, J.M.; Shannon, K.; Butler, B.W. *Simulating Diurnally Driven Slope Winds with WindNinja*; U.S. Department of Agriculture, Forest Service, Rocky Mountain Research Station: Missoula, MT, USA, 2009.
62. Butler, B.W.; Forthofer, J.M.; Finney, M.; McHugh, C.; Stratton, R.; Bradshaw, L. The impact of high resolution wind field simulations on the accuracy of fire growth predictions. *For. Ecol. Manag.* **2006**, *234*, S85. [[CrossRef](#)]
63. Jahdi, R.; Darvishsefat, A.A.; Etemad, V.; Mostafavi, M.A. Wind Effect on Wildfire and Simulation of Its Spread (Case Study: Siahkal Forest in Northern Iran). *J. Agric. Sci. Technol.* **2014**, *16*, 1109–1121.
64. Forthofer, J.M.; Butler, B.W.; McHugh, C.W.; Finney, M.A.; Bradshaw, L.S.; Stratton, R.D.; Shannon, K.S.; Wagenbrenner, N.S. A Comparison of Three Approaches for Simulating Fine-Scale Surface Winds in Support of Wildland Fire Management. Part II. An Exploratory Study of the Effect of Simulated Winds on Fire Growth Simulations. *Int. J. Wildland Fire* **2014**, *23*, 982. [[CrossRef](#)]
65. Horel, J.; Splitt, M.; Dunn, L.; Pechmann, J.; White, B.; Ciliberti, C.; Lazarus, S.; Slemmer, J.; Zaff, D.; Burks, J. Mesowest: Cooperative Mesonets in the Western United States. *Bull. Am. Meteorol. Soc.* **2002**, *83*, 211–226. [[CrossRef](#)]
66. Westerling, A.L.; Cayan, D.R.; Brown, T.J.; Hall, B.L.; Riddle, L.G. Climate, Santa Ana Winds and Autumn Wildfires in Southern California. *Eostransactions Am. Geophys. Union* **2004**, *85*, 289–296. [[CrossRef](#)]
67. Mitchell, J.W. Power Line Failures and Catastrophic Wildfires under Extreme Weather Conditions. *Eng. Fail. Anal.* **2013**, *35*, 726–735. [[CrossRef](#)]
68. Fovell, R.G.; Cao, Y. The Santa Ana Winds of Southern California: Winds, Gusts, and the 2007 Witch Fire. *Wind Struct.* **2017**, *24*, 529–564. [[CrossRef](#)]
69. Cao, Y.; Fovell, R.G. Downslope Windstorms of San Diego County. Part II: Physics Ensemble Analyses and Gust Forecasting. *Weather Forecast.* **2018**, *33*, 539–559. [[CrossRef](#)]
70. Fovell, R.; Gallagher, A. Winds and Gusts during the Thomas Fire. *Fire* **2018**, *1*, 47. [[CrossRef](#)]
71. Santa Barbara County Fire Department. Available online: <https://www.sbcfire.com> (accessed on 10 June 2020).
72. Greig-Smith, P. *Quantitative Plant Ecology*; University of California Press: Berkeley, CA, USA, 1983; Volume 9.
73. Perry, G.L.W.; Sparrow, A.D.; Owens, I.F. A GIS-Supported Model for the Simulation of the Spatial Structure of Wildland Fire, Cass Basin, New Zealand. *J. Appl. Ecol.* **1999**, *36*, 502–518. [[CrossRef](#)]

74. Peterson, S.H.; Morais, M.E.; Carlson, J.M.; Dennison, P.E.; Roberts, D.A.; Moritz, M.A.; Weise, D.R. *Using HFire for Spatial Modeling of Fire in Shrublands*; Research Paper PSW-RP-259; U.S. Department of Agriculture, Forest Service, Pacific Southwest Research Station: Albany, CA, USA, 2009. [[CrossRef](#)]
75. Salis, M.; Ager, A.A.; Arca, B.; Finney, M.A.; Bacciu, V.; Duce, P.; Spano, D. Assessing Exposure of Human and Ecological Values to Wildfire in Sardinia, Italy. *Int. J. Wildland Fire* **2013**, *22*, 549. [[CrossRef](#)]
76. Salis, M.; Arca, B.; Alcasena, F.; Arianoutsou, M.; Bacciu, V.; Duce, P.; Duguy, B.; Koutsias, N.; Mallinis, G.; Mitsopoulos, I.; et al. Predicting Wildfire Spread and Behaviour in Mediterranean Landscapes. *Int. J. Wildland Fire* **2016**, *25*, 1015–1032. [[CrossRef](#)]
77. Stephens, S.L.; Weise, D.R.; Fry, D.L.; Keiffer, R.J.; Dawson, J.; Koo, E.; Potts, J.; Pagni, P.J. Measuring the Rate of Spread of Chaparral Prescribed Fires in Northern California. *Fire Ecol.* **2008**, *4*, 74–86. [[CrossRef](#)]
78. Finney, M.A. *Efforts at Comparing Simulated and Observed Fire Growth Patterns*; Final Report INT-95066-RJVA; Systems for Environmental Management: Missoula, MT, USA, 1998.
79. Fujioka, F.; Chapman University, Orange, CA, USA. Personal communication, 2020.



© 2020 by the authors. Licensee MDPI, Basel, Switzerland. This article is an open access article distributed under the terms and conditions of the Creative Commons Attribution (CC BY) license (<http://creativecommons.org/licenses/by/4.0/>).